Subbarrier fusion of ^{9}Li with ^{70}Zn

W. Loveland,[1] A. M. Vinodkumar,[1] R. S. Naik,[1] P. H. Sprunger,[1] B. Matteson,[1] J. Neeway,[1] M. Trinczek,[2] M. Dombsky,[2] P. Machule,[2] D. Ottewell,[2] D. Cross,[2,4] K. Gagnon,[2,3] and W. J. Mills[2,3]

[1]*Department of Chemistry, Oregon State University, Corvallis, Oregon 97331, USA*

[2]*TRIUMF, Vancouver, British Columbia, Canada V6T 2A3*

[3]*Department of Physics, Simon Fraser University, Burnaby, British Columbia, Canada V5A 1S6*

[4]*Department of Chemistry, Simon Fraser University, Burnaby, British Columbia, Canada V5A 1S6*

(Received 1 September 2006; published 13 December 2006)

The cross section for the fusion of ^{9}Li with ^{70}Zn was measured for seven projectile energies spanning the subbarrier and near-barrier region ($E_{\mathrm{c.m.}}$ ranging from 9.7 to 13.4 MeV) using the ISAC facility at TRIUMF. γ-ray spectroscopy of the irradiated target foils along with β counting of the chemically separated Ge and As evaporation residues were used to measure the fusion cross sections. Statistical model calculations were used to correct for the yields of any unobserved nuclei. The observed fusion excitation function shows significant subbarrier fusion enhancement with a large deduced value of the fusion radius, $R_B = 12.1 \pm 1.0$ fm. Coupled-channels calculations do not account for the observed subbarrier enhancement. The implications of this finding for understanding the fusion of ^{11}Li are discussed.

DOI: 10.1103/PhysRevC.74.064609 PACS number(s): 25.70.Jj, 25.60.Pj, 25.85.−w

I. INTRODUCTION

The nuclear structure and nuclear reactions of ^{9}Li are of interest for three reasons. (a) It is the core nucleus of the two-neutron halo nucleus ^{11}Li that is of great current interest and an understanding of ^{9}Li is important for an understanding of ^{11}Li. (b) ^{9}Li is itself a very neutron-rich nucleus ($N/Z = 2$) with a significant neutron skin [1] and an understanding of its reactions may be helpful in understanding the interactions of very neutron-rich nuclei. (c) ^{9}Li is a well-characterized nucleus with a simple shell-model structure, which should be helpful in modeling its interactions.

In this article, we focus on a study of the fusion excitation function of ^{9}Li interacting with an intermediate mass, neutron-rich nucleus ^{70}Zn. The study was undertaken to gain insight into the fusion of a very neutron-rich projectile with a neutron-rich target nucleus and to serve as a precursor of a study of the fusion of ^{11}Li with this nucleus.

Previous studies have been made, at intermediate energies, of the elastic scattering of ^{9}Li [2] and the total interaction cross section of ^{9}Li interacting with intermediate mass nuclei, such as Cu [3]. Both nuclear interactions and electromagnetic dissociation were observed with the interaction radius of ^{9}Li being normal. The fusion of ^{9}Li with Si at 11.2 A–15.2 A MeV was studied at RIKEN [4] by measuring the evaporation residues and any associated neutrons. In contrast to similar studies with ^{11}Li, the neutron spectra associated with the ^{9}Li interactions had the shape of fusion evaporation spectra. However, no detailed information on the fusion cross sections or an analysis of them is available. The fusion of ^{9}Li with ^{209}Bi (at a projectile energy of 36 MeV) was also studied at RIKEN [5]. The ratio of the production cross sections for the evaporation residues ^{214}Rn and ^{215}Rn was measured but no fusion cross section was measured.

With this in mind, we undertook a study of the fusion of ^{9}Li with ^{70}Zn at the ISAC facility at TRIUMF. [We also attempted, unsuccessfully (see Appendix), to measure the fusion cross section of ^{11}Li interacting with ^{70}Zn.] In Sec. II of this article, we describe the experimental apparatus; our results are presented and discussed in Sec. III. Conclusions are given in Sec. IV.

II. EXPERIMENTAL METHODS

The measurement of the fusion cross sections for the ^{9}Li+^{70}Zn reaction was carried out at the ISAC facility at TRIUMF. Proton beams (500 MeV) with intensities ranging from 50–85 μA struck Ta metal production targets. Beams of radioactive ^{9}Li were extracted with energies up to 18.4 keV, mass separated by passage through two dipole magnets and accelerated to their final energy by radiofrequency quadrupole and drift tube linear accelerators. The details of the production of these secondary beams are discussed elsewhere [6,7].

After acceleration, the beam was delivered to the HEBT straight-through beam line in the ISAC facility. The experiment was carried out in a large-volume (∼40 L) scattering chamber, known as the Laval chamber, at the end of this beam line. The beams struck ^{70}Zn targets mounted in the chamber. Beam intensities were monitored by detecting elastic scattering at $\pm 16.2^{\circ}$ with additional monitoring of the beam by a suppressed Faraday cup at the end of the beam line. The experiments were carried out in two separate runs, August–September 2005 and May–June 2006. In the 2005 experiments, the primary proton beam was 50 μA and the average on-target ^{9}Li intensity was 5×10^{6} particles/s. In the 2006 experiments, higher proton currents were used (50–85 μA) and the average on-target beam intensity was slightly less, 4×10^{6} particles/s.

^{70}Zn was chosen as the target for this study because of its neutron-richness and because the predicted evaporation residues (As or Ge nuclei) were easily detected using radiochemical techniques and because it is possible to get above the interaction barrier with the ISAC ^{9}Li beam, which has

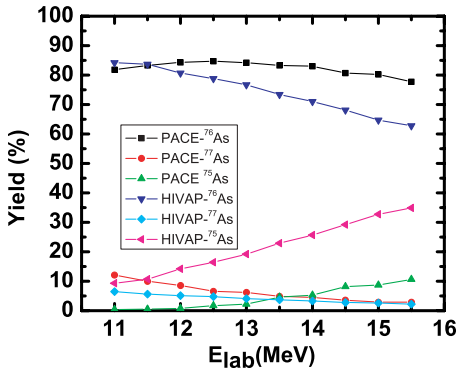

FIG. 1. (Color online) Statistical model simulations of the expected yields of various nuclides in the reaction of ^{9}Li with ^{70}Zn.

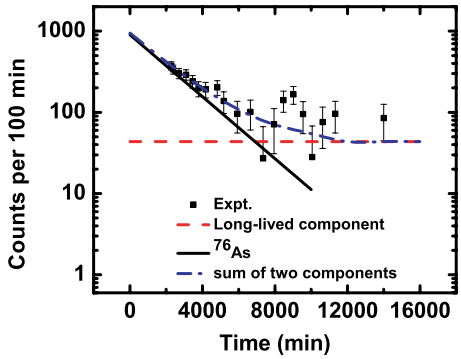

FIG. 2. (Color online) Decay curve for β counting of As chemical fraction from the reaction of 14.7 MeV ^{9}Li+^{70}Zn. The decay curve is resolved into two components: that due to ^{76}As decay (solid line) and that due to a long-lived background activity (dashed line). The sum of the two components is shown as a dash-dotted line.

a maximum energy of ∼1.71 A MeV. Targets of ∼95% enriched ^{70}Zn (thickness ∼0.8–1.1 mg/cm^2) were prepared by electrodeposition on Al backing foils (0.54–0.71 mg/cm^2).

Si detectors (300 mm^2) were mounted ∼40 cm from the target at ±16.2° to monitor the ^{9}Li elastic scattering during each irradiation. Another measure of the beam intensity was a shielded, suppressed Faraday cup at the end of the beam line, which agreed roughly with the Rutherford scattering estimates of the beam doses. ^{9}Li is 178 ms β emitter with a $Q_\beta \sim 13.6$ MeV with ∼50% of the decays resulting in neutron emission. Because we were not sure how the Faraday cup would respond to the high-energy β decays, we chose Rutherford/elastic scattering as the primary monitor of the beam intensity. A 0.008-m^3 shield of 5% boron-loaded paraffin was used to reduce the neutron emission from the Faraday cup to acceptable levels.

Before discussing the results of the measurement of the evaporation residue yields, it might be useful to discuss what we might expect. In Fig. 1, we show the predicted cross sections for the various nuclides formed in this reaction. These simulations were done using the statistical model codes PACE v. 4.13 [8] and HIVAP [9]. The entire evaporation residue cross section is predicted to be concentrated in the three isotopes of As, stable ^{75}As, 1.09-day ^{76}As, and 38.8-h ^{77}As. Both simulations show the largest predicted component is ^{76}As. ^{77}As, a minor component of the yield, has the further complication that its β branch to the excited states of the daughter is small, causing the characteristic decay γ-ray line at 239 keV to be present in only 1.6% of the decays.

For each of the ^{9}Li energies studied, a fresh ^{70}Zn target was installed in the scattering chamber and it was irradiated for 1–3 days. In the 2006 run, the irradiated target foil was counted with a Ge γ-ray spectrometer for about 1 day prior to commencing a radiochemical analysis of the target. The Ge γ-ray spectrometer consisted of a large-volume Ge detector (efficiency ∼80% of NaI) connected to digital signal processing electronics (ORTEC DSPEC). The efficiency of the detector was measured with NIST calibrated γ-ray standards. The γ-ray spectra were analyzed using DECHAOS [10] to give absolute end of bombardment activities. Cross sections were calculated for the observed residue nuclei taking into account the temporal variation of the beam intensity during the irradiations.

Following γ-ray spectroscopy, the irradiated target foil and backing material were dissolved in acid and the As and Ge residues were separated by standard radiochemical separations [11]. Then the As and Ge fractions were assayed using a Tennelec LB1000 Low Background Beta Counter (efficiency ∼52.5%) and the decay of the sample was followed for several days. The yields of the As chemical separation ranged from 27 to 100% (average yield = 63%), whereas the yields of the Ge separations ranged from 3 to 32% (average yield = 22%). (These yields were determined by post irradiation neutron activation analysis of the samples.) The residue nuclei were identified by their atomic number (established by chemistry) and their observed decay half-life.

The decay curves for the β counting were resolved using the DECHAOS software. A typical decay curve is shown in Fig. 2. The only detected activity in any irradiation was ^{76}As. Upper limits (2σ) for the production of ^{77}Ge and ^{77}As were ∼0.1 mb. After correction for chemical yields, branching ratios, detector efficiency, temporal variation of the beam intensity during the irradiations, etc., the production cross sections for the residue nuclei were calculated.

In Table I, we summarize the details of each irradiation. ($E_{\rm cot}$ is the center-of-target beam energy.) Where a cross section was determined by both γ-ray spectroscopy and β counting, the results were averaged to get the final cross section. To get the fusion cross sections from the observed radionuclide yields, a correction for unobserved products must

TABLE I. Details of the ^{9}Li irradiations.

$E_{\rm lab}$ (MeV)	$E_{\rm cot}$ (MeV)	$t_{\rm irr}$ (min)	Dose (particles)	Method of assaying samples
11.5	11.0	848	3.4×10^{11}	β
12.5	12.0	5099	2.6×10^{11}	β, γ
13.5	13.0	1006	2.3×10^{11}	β
14.0	13.7	2395	6.5×10^{11}	β, γ
14.5	14.1	2577	5.9×10^{11}	β, γ
15.1	14.7	2062	4.2×10^{11}	β, γ
15.4	15.0	1196	3.9×10^{11}	β

TABLE II. Measured fusion cross sections for the reaction of ^{9}Li with ^{70}Zn.

E_{cot} (MeV)	$E_{c.m.}$ (MeV)	Cross section (mb)
11.0	9.7	34.1 ± 6.6
12.0	10.6	51.7 ± 23.1
13.0	11.5	79.2 ± 12.1
13.7	12.1	178.1 ± 16.7
14.1	12.5	214.8 ± 15.6
14.7	13.	391.3 ± 22.3
15.0	13.4	341. ± 36.3

be made. That correction was taken as the average value of the ratio of the fusion cross section to the ^{76}As production cross section as computed using the statistical model codes PACE v. 4.13 [8] and HIVAP [9]. These corrections ranged from 0.72 to 0.83 for the different projectile energies.

III. RESULTS AND DISCUSSION

The observed fusion cross sections are tabulated in Table II and plotted as a function of beam energy in Fig. 3. The uncertainties in the cross sections reflect the uncertainties in the measured activities (primary uncertainty) and the systematic uncertainties, such as detector efficiencies, beam integration, decay branching ratios, correction for missing activities, etc.

To place these data in the context of other similar measurements of fusion excitation functions for Li interacting with Zn, we show in Fig. 4 the reduced fusion excitation functions for the ^{6,7}Li+^{64}Zn [12] and the ^{9}Li+^{70}Zn reactions. In making this plot we divided the center-of-mass (c.m.) beam energy by the value of the fusion barrier height, V_B, for each system as derived from the semiempirical Bass model [13] and divided the cross section by the square of the Bass model fusion radius, R_B. (Use of another semiempirical prescription [14] for V_B and R_B would change the values of the scaling parameters by 3–4%.) We see, immediately, that the projectile energies used in this work are sub- and near barrier, whereas the studies with ^{6,7}Li were at a much higher energy. The Bass model barrier

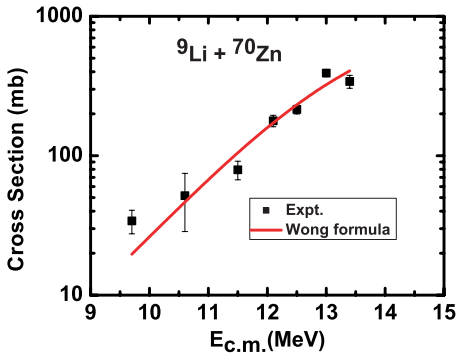

FIG. 3. (Color online) The measured fusion excitation function for the ^{9}Li+^{70}Zn reaction. The line is the result of fitting the data with the Wong one-dimensional barrier penetration model with V_B = 12.5 MeV, R_B = 12.1±1.0 fm, and $\hbar\omega$ = 5.7±0.8 MeV.

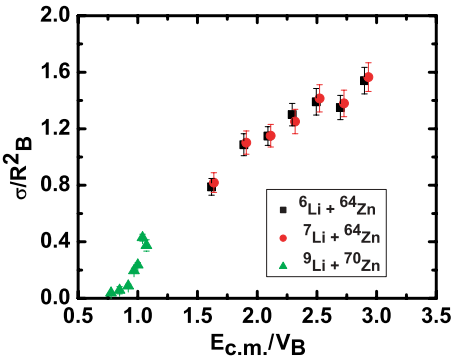

FIG. 4. (Color online) The reduced fusion excitation functions for the reaction of ^{6,7}Li with ^{64}Zn and ^{9}Li with ^{70}Zn.

height for the ^{9}Li+^{70}Zn system is 12.5 MeV, with most of our data being taken in the subbarrier region.

To describe this subbarrier fusion, we anticipate that the nuclear structure of ^{9}Li will be important. ^{9}Li has a charge radius, r_c = 2.217 fm [15], a matter radius of 2.44± 0.08 fm [16], and a neutron radius of 2.59 fm [16]. As such, the nucleus is described [16] as having a neutron skin of thickness 0.48 fm. The density distribution for ^{9}Li, although not as large as for ^{11}Li, does show a significant tail to large radii with $\rho = 10^{-4}$ nucleon/fm^3 at 6.5 fm [17]. ^{9}Li has been described in the shell model [18] as a combination of ^{4}He, ^{3}H, and two neutrons. The Q value for two-neutron transfer (^{9}Li + ^{70}Zn → ^{7}Li + ^{72}Zn) is large (+8.612 MeV). All of these factors lead us to expect a large fusion radius for ^{9}Li involving the interaction of the skin neutrons with neutron-rich ^{70}Zn.

A simple way to demonstrate this effect numerically is through the use of the Wong formula [19]. The Wong formula represents the fusion barrier as a parabola and, in a semiclassical expression, describes the fusion cross section, σ_W, as

$$\sigma_W = \frac{\hbar\omega_B R_B^2}{2E} \ln\left\{1 + \exp\left[\frac{2\pi}{\hbar\omega_B}(E - V_B)\right]\right\} \qquad (1)$$

in terms of the fusion barrier height V_B, fusion radius R_B, and barrier curvature $\hbar\omega_B$. We fixed the value of V_B at 12.5 MeV [13] and fit the data by varying R_B and $\hbar\omega_B$ giving values of R_B = 12.1 ± 1.0 fm and $\hbar\omega_B$ = 5.7±0.8 MeV. The data are well described (Fig. 3). (Allowing all parameters to vary produced R_B = 18±29 fm, V_B = 13.8±4.9 MeV, and $\hbar\omega_B$ = 6.8±2.5 MeV. Because that fit is not statistically meaningful, we constrained V_B to be the value represented by the semiempirical Bass model.) The deduced value of R_B, 12.1 fm, is substantially larger than the simple touching radius ($2.44 + 1.2 \times 70^{1/3} = 7.44$ fm) and presumably reflects the interaction of the large tail of the ^{9}Li density distribution with that of ^{70}Zn. ^{9}Li is moderately deformed ($\beta_2 = -0.235$) [18], whereas ^{70}Zn has $\beta_2 = 0.228$ [20].

It is traditional to evaluate subbarrier fusion cross sections, such as those measured in this work, using a coupled-channels calculation. We used the code CCFULL [21] to make this calculation. We included the inelastic excitation of the first vibrational 2+ and 3− states in ^{70}Zn [20] and the rotational states in ^{9}Li [20]. We assumed a potential with

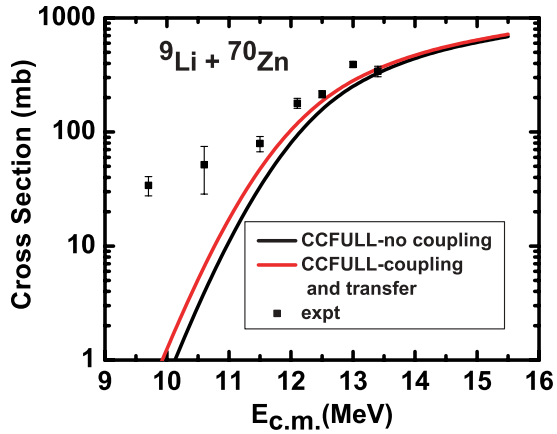

FIG. 5. (Color online) Comparison of the measured fusion excitation function for the ^{9}Li+^{70}Zn reaction and the predictions of a coupled-channels calculation.

$V_0 = 105$ MeV, $r_0 = 1.12$ fm and a diffuseness parameter $a = 0.65$ fm. We also included the two-neutron transfer channel described earlier (coupling strength = 0.3). In Fig. 5, we compare the measured data with the CCFULL calculations. There is a large subbarrier fusion enhancement that is not described by the coupled-channels calculation.

It is clear that the subbarrier fusion of ^{9}Li is not easily described in conventional models of fusion. What are the consequences of this for understanding the fusion of ^{11}Li? As a schematic illustration of the difficulties posed by the data measured in this work, we show, in Fig. 6, the fusion excitation function for ^{9}Li+^{70}Zn "scaled up" to the ^{9}Li+^{208}Pb reaction. To do the "scaling," we have simply assumed the reduced excitation functions for the two systems are the same, and scaled projectile energies by the Bass barrier heights and the cross sections by the Bass model fusion radii. We also show a sample theoretical calculation of the expected fusion cross section associated with the fusion of ^{9}Li with ^{208}Pb [22]. The observed subbarrier fusion enhancement is not predicted and if this enhancement occurs for the fusion of the ^{9}Li core in the ^{11}Li reactions, it will complicate the description of these

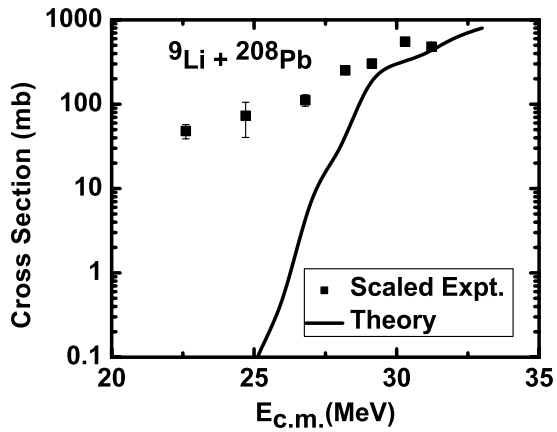

FIG. 6. Schematic comparison of the fusion excitation function for the ^{9}Li+^{208}Pb reaction as scaled from the data measured in this experiment and a calculation [22] of this excitation function.

reactions. For example, the central issue in the fusion of ^{11}Li with ^{208}Pb [23] is the effect of the breakup of ^{11}Li prior to fusion. One measure of whether this occurs is the observation of subbarrier fusion enhancement, i.e., if no breakup occurs, one expects [23] that the subbarrier fusion of ^{11}Li with ^{208}Pb will be greatly enhanced by the halo nucleons. But if the ^{9}Li core already shows this subbarrier fusion enhancement independent of the presence or absence of the halo nucleons, determining the effect of the breakup of ^{11}Li will be more difficult.

IV. CONCLUSIONS AND SUGGESTIONS FOR FUTURE WORK

What have we learned from this study? We conclude that: (a) It is possible to measure fusion excitation functions for light and intermediate mass nuclei using current ^{9}Li radioactive beams. (b) The fusion excitation function for the ^{9}Li+^{70}Zn reaction shows a large subbarrier fusion enhancement that is not accounted for by current coupled channel calculations. (c) The large fusion radius, $R_B = 12.1 \pm 1.0$ fm, deduced from fitting the observed excitation function may be due to the neutron skin and extended neutron density distribution of ^{9}Li. (d) The analysis of ^{11}Li fusion reactions will need to take into account the unexpected subbarrier fusion enhancement associated with the ^{9}Li core.

Possible extensions of this work include: (a) actually performing the study of the fusion of ^{9}Li with ^{208}Pb to verify that the behavior predicted by excitation function scaling actually occurs and (b) extension of future studies of the fusion of ^{9}Li to lower energies to determine the limits of the subbarrier fusion.

ACKNOWLEDGMENTS

We thank the operations staff of the cyclotron and ISAC, in particular, Chris Payne and Marco Marchetti, for providing the ^{9}Li beams. This work was supported in part by the Director, Office of Energy Research, Division of Nuclear Physics of the Office of High Energy and Nuclear Physics of the U.S. Department of Energy under grant DE-FG06-97ER41026 and TRIUMF and the Natural Sciences and Engineering Research Council of Canada.

APPENDIX

One of the original goals of this experiment was to measure the fusion excitation function for the ^{11}Li+^{70}Zn reaction.

TABLE III. Details of the ^{11}Li irradiations.

E_{lab} (MeV)	E_{cot} (MeV)	t_{irr} (min)	Dose (particles)
17.5	17.0	2546	1.04×10^8
17.5	17.0	3647	2.16×10^8
16.5	16.1	2840	7.78×10^7

TABLE IV. Measured upper limit (2 σ) cross sections for the ^{11}Li+^{70}Zn reaction.

E_{lab} (MeV)	Upper limit cross section (b)
17.5	31
17.5	27
16.5	55

Three separate irradiations of ^{70}Zn targets with beams of ^{11}Li were made in hopes of detecting evaporation residues. The ^{11}Li beams were produced in a similar manner to that described for the production of ^{9}Li beams. Proton beam currents of 50 μA (2005) and 100 μA (2006) were used to produce ^{11}Li beams. The average on-target beam intensities were 680 particles/s (2005) and 740 particles/s (2006). At these incident beam intensities, detection of evaporation residues, even using sensitive radiochemical techniques, is difficult.

The details of the irradiations are given in Table III. Following each irradiation, the ^{70}Zn targets and backing foils were dissolved in acid and As and Ge chemical fractions were isolated using the same methods employed in the ^{9}Li irradiations. Upper limits on cross sections were calculated for each irradiation and are summarized in Table IV. The values of these upper limits are so large as to be meaningless. The currently available energetic ^{11}Li beams are not sufficiently intense to do studies of fusion reactions.

[1] G. F. Bertsch, B. A. Brown, and H. Sagawa, Phys. Rev. C **39**, 1154 (1989).
[2] D. Peterson, J. J. Kolata, P. Santi, J. von Schwarzenberg, D. Bazin, and B. M. Sherrill, Phys. Rev. C **67**, 014601 (2003).
[3] B. Blank *et al*., Nucl. Phys. **A555**, 408 (1993).
[4] M. Petrascu *et al*., Phys. Lett. **B405**, 224 (1997).
[5] A. Yoshida *et al*., in *Heavy Ion Fusion: Exploring the Variety of Nuclear Properties*, edited by A. M. Stefanini, G. Nebbia, S. Lunardi, and G. Montagnoli (World Scientific, Singapore, 1994), pp. 311–318.
[6] P. Bricault, M. Dombsky, A. Dowling, and M. Lane, Nucl. Instrum. Methods Phys. Res. B **204**, 319 (2003).
[7] M. Dombsky, P. Bricault, and V. Hanemaayer, Nucl. Phys. **A746**, 32c (2004).
[8] O. B. Tarasov and D. Bazin, Nucl. Instrum. Methods Phys. Res. B **204**, 174 (2003).
[9] W. Reisdorf, Z. Phys. A **300**, 227 (1981).
[10] K. Aleklett, J. O. Liljenzin, and W. Loveland, J. Radioanal. Nucl. Chem. **193**, 187 (1995).
[11] NAS-NS-3002(rev), Radiochemistry of Arsenic, p. 34 (1965).
[12] I. Padron *et al*., Phys. Rev. C **66**, 044608 (2002).
[13] R. Bass, *Nuclear Reactions with Heavy Ions* (Springer, New York, 1980).
[14] L. C. Vaz, J. M. Alexander, and G. R. Satchler, Phys. Rep. **69**, 373 (1981).
[15] R. Sanchez *et al*., Phys. Rev. Lett. **96**, 033002 (2006).
[16] A. V. Dobrovolsky *et al*., Nucl. Phys. **A766**,1 (2004).
[17] A. Bhagwat, Y. K. Gambhir, and S. H. Patel, J. Phys. G **27**, B1 (2001).
[18] D. Borremans *et al*., Phys. Rev. C **72**, 044309 (2005).
[19] C. Y. Wong, Phys. Rev. Lett. **31**, 766 (1973).
[20] The energy levels for the nuclei in question were taken from the ENSDF files at the National Nuclear Data Center (http://www.nndc.bnl.gov), whereas the deformations were taken from S. Raman, C. W. Nestor, and P. Tikkanen, At. Data Nucl. Data Tables **78**, 1 (2001); R. H. Spear, At. Data Nucl. Data Tables **42**, 55 (1989).
[21] K. Hagino, N. Rowley, and A. T. Kruppa, Comput. Phys. Commun. **123**, 143 (1999).
[22] N. Takigawa, M. Kuratani, and H. Sagawa, Phys. Rev. C **47**, R2470 (1993).
[23] C. Signorini, Nucl. Phys. **A693**, 190 (2001).